Journal of the Nigerian Association of Mathematical Physics
Volume 51 (*May, 2019 Issue*), pp177 – 186

SHELL MODEL CALCULATIONS WITH TENSOR CORRELATIONS EFFECT ON THE POSITIVE PARITY STATES OF THE EVEN-EVEN NUCLEI IN THE SD-SHELL

F. Gbaorun[1],J. O. Fiase[1]and J. T. Ikyumbur[2]

[1]Department of Physics, Benue State University, P. M. B. 102119,Makurdi, Benue State, Nigeria.
[2]Department of Physics, Federal College of Education, Pankshing, Plateau State, Nigeria.

Abstract

Effects of tensor correlations on the positive parity states of even-even nuclei in the sd shell are examined. Two-body nuclear matrix elements are obtained by the lowest order constrained variational technique with and without tensor correlations. The matrix elements calculated are used as input into the NUSHELL shell model code to calculate the energy spectra of all the even-even nuclei with and without tensor correlations in the sd-shell region. We have found that the effects of tensor correlations is to open up the calculated energy spectra and provide reasonable agreement with experiment, whereas the energy spectra calculated without tensor correlations compress the energy spectra and provide significant disagreement with experimental data. The results presented here re-emphasize the strong evidence found in nuclear structure calculations that tensor correlations are very important in nuclei and their presence cannot be ignored.

***Keywords*:** Shell Model Calculation, sd-Shell, Tensor Correlations, NUSHELL Code, Energy Spectra, Even-Even nuclei.

1.0 Introduction.

In the rest-frame of the nucleus, the non-relativistic many nucleon Hamiltonian incorporating pairwise interactions can be written as [1]

$$H = \sum_{i>j}\left[p_{ij}^2 / M(A) + V_{ij}\right], \tag{1}$$

where $\underline{p_{ij}}$ is the relative momentum, $\underline{p_{ij}} = \frac{1}{\sqrt{2}}\left(\underline{p_i} - \underline{p_j}\right)$, $M(A) \approx m_N A$ is the total mass of the nucleons while V_{ij} is taken here to be the Nijmegen potential [2]. An effective Hamiltonian can be defined which takes the form [3,4]:

$$H_{eff} = \sum_{i>j} f_{ij}\left(\frac{p_{ij}^2}{M} + V_{ij}\right) f_{ij}, \tag{2}$$

where the f_{ij} are two-body correlation operators. In earlier studies regarding nuclear matter and finite nuclei [4], the two-body correlation functions were found to have three features. These included (i) the "wound" induced in the two - body wave function by the repulsive core of the NN interaction; (ii) the tensor correlations especially in the ${}^3S_1 - {}^3D_1$ channel and; (iii) the meson exchange corrections. The most important of these features was found to be the tensor correlations, hence, the two-body correlation functions were parameterized in the form [5,6]

$$\begin{aligned} r_{ij} < r_c \quad &: \quad f_{ij} = 0 \\ r_{ij} > r_c \quad &: \quad f_{ij} = f(r_{ij})\sum_{\lambda}\left(1 + \alpha_\lambda(A) S_{ij}\right) \end{aligned} \tag{3}$$

where the sum λ is over all reaction channels and $f(r_{ij})$ is parameterized as:

Corresponding Author**:** Gbaorun F., Email: fredgbaorun@gmail.com, Tel: +2347038635405

$$f(r_{ij}) = 1 - \exp[-\beta(r_{ij} - r_c)^2] \quad (4)$$

In Eq. (4), $r_c = 0.25\ fm$ and $\beta = 25\ fm^{-2}$ which represents the short-range repulsion of the bare NN interaction, S_{ij} is the usual tensor operator; $\alpha_\lambda(A)$ is the strength of the tensor correlations which is measured by the condition:

$$\alpha_\lambda(A)\left(\equiv 0,\ \lambda \neq {}^3S_1 - {}^3D_1\right). \quad (5)$$

It should be noted that in this paper we have used a simple form of the two-body correlation functions. More sophisticated sets of two - body correlation functions are in use and are designed to be different in different partial waves. This present choice has been used because it is particularly suitable in studying the effects of tensor correlations on energy spectra of nuclei as this can be done by simply switching 'on' and 'off' the strength of the tensor correlations, $\alpha_\lambda(A)$.

Some years ago [7] we presented the above prescription for calculating an effective interaction in the rest-frame of the nucleus. We used the Reid Soft-Core potential. However, we did not calculate the energy spectra of corresponding nuclei with our interaction. We only compared our work with other fitted interactions. In this work we repeat our earlier prescription but this time we have calculated the energy spectra of selected nuclei with the more modern Nijmegen potential [2]. Our motivation in this work is to investigate the effects of tensor correlations on energy levels of all the even nuclei in the sd-region and compare with the results of other workers [8-12]. To the best of our knowledge, a study on the interplay of energy levels and tensor correlations has not been investigated.

The paper is divided as follows: In Section 2, we compare the matrix elements of the present interaction with those fitted to experimental data by Wildenthal [13]. In Section 3 we present the results of the variance between our matrix elements and those of Wildenthal [8]. In Section 4 we present the spectra of the energy levels of nuclei under question. Section 5 is concerned with summary and conclusion.

2. Comparison of the Matrix Elements.

The matrix elements of Eq.(2) were calculated in a harmonic oscillator basis. In calculating the matrix elements, we have only two free parameters to vary. These are the strength of the tensor correlations defined by $\alpha_\lambda(A)$ described earlier and the oscillator size parameter $\hbar\omega(A)$ contained in the wave function. As already discussed, the aim of this paper is to show the effect of tensor correlations induced by the tensor force component in V_{ij} on the energy spectra of nuclei. We do this by varying the strength of the tensor correlations as follows: By setting $\alpha_\lambda(A) = 0$, we have no tensor correlations. However, if we let $\alpha_\lambda(A)$ assume a finite value, then we have tensor correlations.

We next compared the calculated matrix elements described by the two conditions of $\alpha_\lambda(A)$ above with the fitted interaction of Wildenthal [13]. It should be noted that the interaction described by Wildenthal [12] has been fitted to experimental data for nuclei in the range $18 \leq A \leq 40$ and it is mass dependent. The present interaction is also mass dependent through $\alpha_\lambda(A)$, Eq. (1) and $\hbar\omega(A)$.

In ref. [7] it was found that the comparison between our matrix with those fitted to experimental data was good only to a constant shift, Δ to the diagonal matrix elements. We have repeated the same analysis here and have found similar results.

In Figures 1.1 to 1.4, we present the T = 1 and T = 0 diagonal and non - diagonal two-body matrix elements for the A = 20 system for the present calculation and those of Wildenthal [13]. Figures 1.1 and 1.2 show the results when the strength of the tensor correlations is switched off i.e. $\alpha_\lambda(A) = 0$ (no tensor correlations) while Figures 1.2 and 1.4are the results when $\alpha_\lambda(A)$ takes on a finite value ($\alpha_\lambda(A) = 0.0550$ in this case). In the case of Figure 1.1 (tensor correlations switched off) we have applied a constant shift of Δ = 2.5 MeV to all the diagonal matrix elements while in Figure 1.4 (tensor correlations switched on) a constant shift of Δ = 2.4 MeV has been applied to all the diagonal matrix elements.

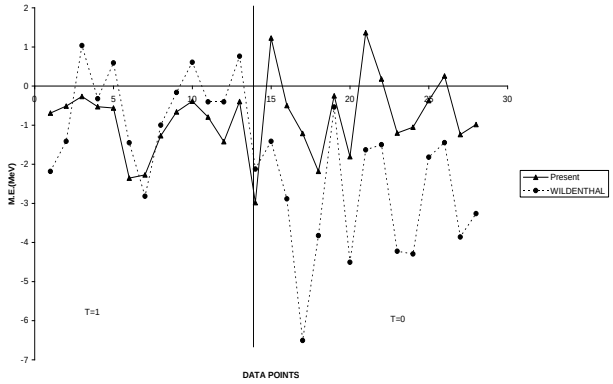

Figure 1. 1T = 1 and T = 0 diagonal matrix elements for the present calculation and Wildenthal's with $\alpha_\lambda(A) = 0.0000$, A = 20, $\hbar\omega = 13$ and Δ = 2.5 MeV . Doted lines represent Wildenthal's matrix elements while the solid lines are the present calculations.

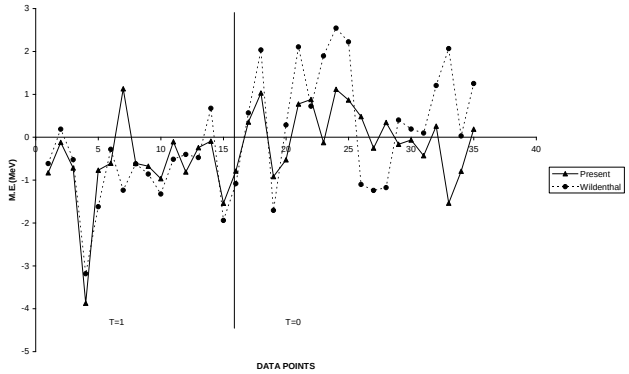

Figure 1.2. T = 1 and T = 0 non-diagonal matrix elements for the present calculation and Wildenthal's with, $\alpha_\lambda(A) = 0.0000$, $A = 20$ and $\hbar\omega = 13$.

Doted line represent Wildenthal's matrix elements while the solid lines represent the present calculation.

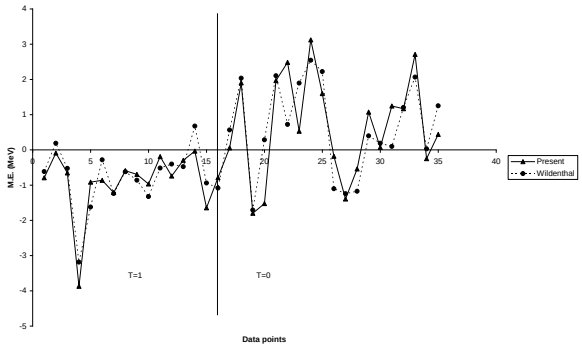

Figure 1.3. T = 1 and T = 0 non-diagonal matrix elements for the present calculation and Wildenthal's with $\alpha_\lambda(A) = 0.0550$, $A = 20$, and $\hbar\omega = 13$.

Doted line represents Wildenthal's matrix elements while the solid line represents present calculation.

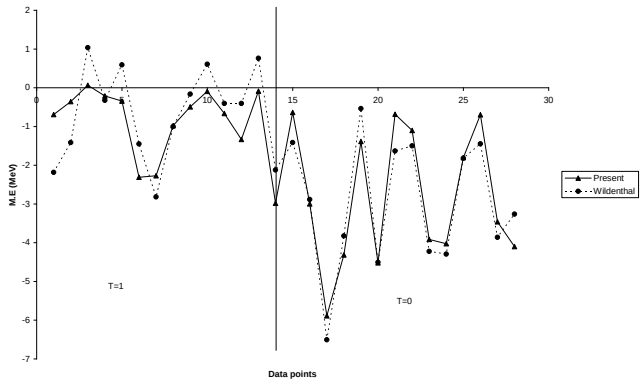

Figure 1.4T = 1 and T = 0 diagonal matrix elements for the present calculation and Wildenthal's with $\alpha_\lambda(A) = 0.0550$, $A = 20$,Δ = 2.4MeVand $\hbar\omega = 13$.Solid lines represent Wildenthal's matrix elements while the doted lines represent present calculation

3. Results of the Variance

In Figures 2.1 – 2.8, we present the variance of our calculated matrix elements with those of the fitted interaction of Wildenthal [13]. We define the variance in the form

$$\chi = \frac{\sum_i^{63}\left(ME_i^F - ME_i^C\right)^2}{\left(\sum_i^{63} ME_i^F\right)^2}, \qquad (5)$$

where the sum is over the sixty-three two-body matrix elements. In Eq.(5), ME_i^F are the two-body matrix elements of the fitted interaction while ME_i^C are those of the present interaction.

In Figure 2.1the variance χ is plotted for $\hbar\omega = 11$, and $\alpha = 0.0550$ as a function of the shift in the diagonal two-body matrix elements, Δ. We have found that for every mass number, A, an optimized variance can be found which brings our calculated two-body matrix elements in line with the fitted data of Wildenthal.

In the present choice the value of the optimized variance is, $\chi \approx 0.1$. On the other hand, by repeating the above procedure and switching off the strength of the tensor correlations, as in Figure 2.2, the variance went up to $\chi \approx 0.5$, showing a poor agreement with the fitted interaction of Wildenthal. We have repeated the same procedure in Figures 2.3, 2.4, 2.5, 2.6, 2.7 and 2.8 for different values of $\hbar\omega$ and $\alpha_\lambda(A)$, and have found similar trend.

4. The Energy Spectra.

In Figures 3.1 – 3.7, we plot the calculated energy spectra of even-even nuclei in the range $18 \le A \le 40$ with and without the effect of tensor correlations. Figure3.1. isthe ^{18}F spectrum. In this Figure, the lowest five experimental energy levels are reproduced with tensor correlations switched on. However, the energy spacing are higher than their experimental counterparts. In fact, the first $0^+1$and the first 5^+0 levels have actually interchanged order.On the other hand, we cannot assign any of the experimental energy levels with the calculated energy levels when tensor correlations are turned off. Also comparison with other workers [14] shows poor agreement when Tensor correlations are turned off.

The spectrum of ^{20}Ne is depicted in Figure 3.2.The first five experimental energy levels are well reproduced when tensor correlations are switched on. On the other hand the same levels are also reproduced but the spectrum is somehow compressed when tensor correlations are switched off. Similar trend is observed in Figure.3.3 which shows the ^{24}Mg spectrum. Here, the first six experimental levels are reproduced when tensor correlations are switched on except that the second 2^+ state interchanges sign with the first 4^+ state. On the other hand, the effect of switching off the tensor correlations compresses the spectrum and the agreement with experiment is poor.

In Figure 3.4 wherethe ^{28}Si spectrum is plotted, the first four experimental energy levels are well reproduced when tensor correlations are switched on. The pattern obtained here for this nucleus is similar with the works other researchers [15–17]. However, the calculated spectrum is severely compressed when tensor correlations are switched off, and agreement with the experimental spectrum becomes very poor.

As can be seen from our calculations pictorially illustrated in Figure 3.5 which presents ^{32}S spectrum, the energy levels are not well reproduced on a one-to-one basis for ^{32}S nucleus even when tensor correlations are switched on. However, as can be seen, switching on the tensor correlation opens up the spectrum while switching off the tensor correlations compresses the spectrum.

The description of ^{36}Ar Spectrum is given in Figure 3.6.The first six experimental levels are confirmed to be reproduced with tensor correlations switched on [17]. However, the first 4^+ and the first 0^+ levels have interchanged order. On the hand, the same spectrum in question is compressed when tensor correlations are switched off. Finally, the last nucleus investigated in the present work is Potassium ^{38}K with its calculated spectrum depicted in Figure 3.7. The lowest five experimental energy levels are reproduced with tensor correlations switched on. On the other hand we cannot assign correctly any of the experimental energy levels with our calculated spectrum when tensor correlations are switched off.

5. Summary and Conclusion.

The study of the interplay of the various components of the nuclear force on measurable quantities such as the energy levels of nuclei is not an easy one. In this work we have studied the effect of the tensor correlations induced by the repulsive core of the NN force on the energy spectra of even - even nuclei in the range $18 \le A \le 40$. We have found that the strength of the tensor correlations is very important in obtaining reasonable agreement with experiment. Indeed we have found that when the strength of tensor correlations are switched off, the calculated energy spectrum either compress very severely or disagrees significantly with experiment. We expect to find the same kind of trend on measurable quantities when studying astrophysical quantities where tensor correlations are involved.

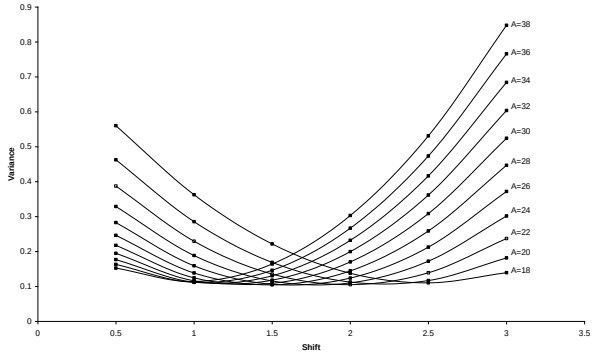

Figure 2.1 Graph of variance χ for $\hbar\omega = 11$, and $\alpha = 0.0550$ as a function of shiftΔ in the diagonal two-body matrix elements

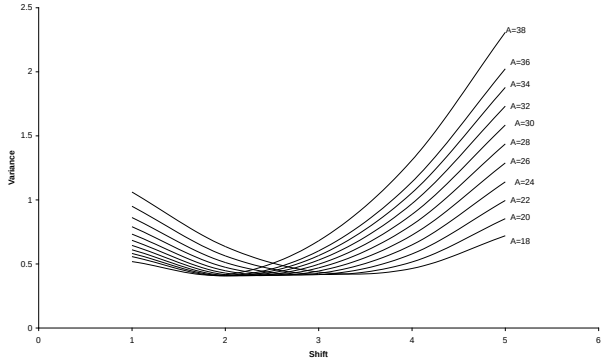

Figure 2.2 Graph of variance χ for $\hbar\omega = 11$, and $\alpha = 0.0000$ as a function of shiftΔ in the diagonal two-body matrix elements

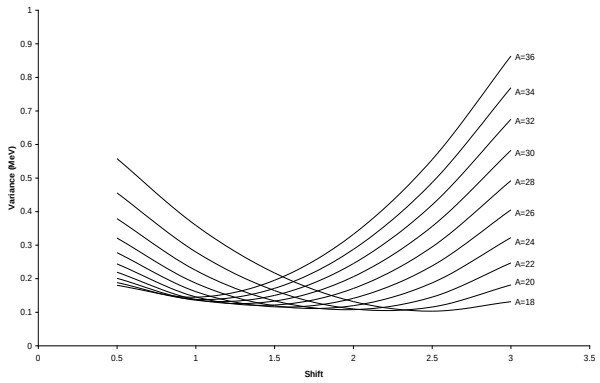

Figure 2.3 Graph of variance χ for $\hbar\omega = 12$, and $\alpha = 0.0600$ as a function of the shift Δ in the diagonal two-body matrix elements

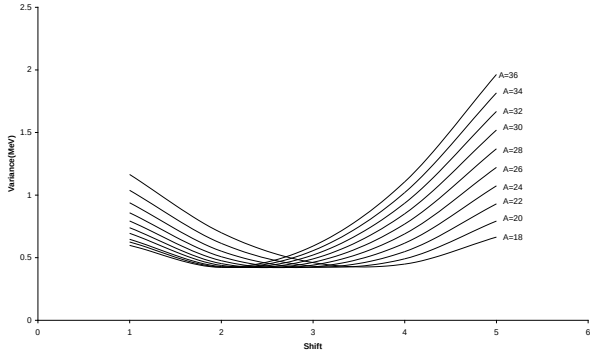

Figure 2.4 Graph of variance χ for $\hbar\omega = 12$, and $\alpha = 0.0000$ as a function of shift Δ in the diagonal two-body matrix elements

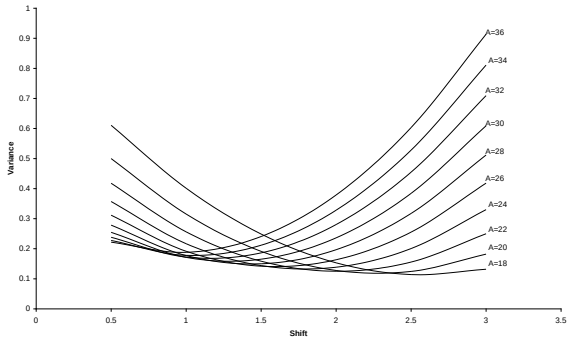

Figure 2.5 Graph of variance χ for $\hbar\omega = 13$, and $\alpha = 0.0600$ as a function of shift Δ in the diagonal two-body matrix elements

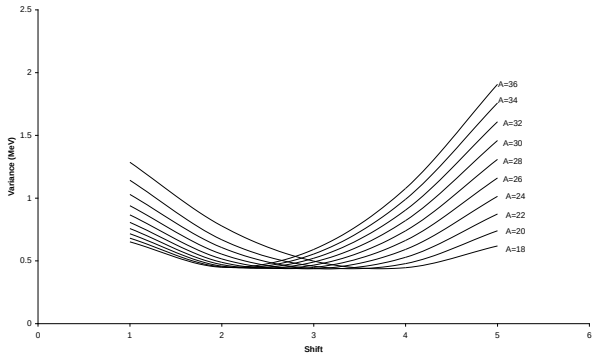

Figure 2.6 Graph of variance χ for $\hbar\omega = 13$, and $\alpha = 0.0000$ as a function of shift Δ in the diagonal two-body matrix elements

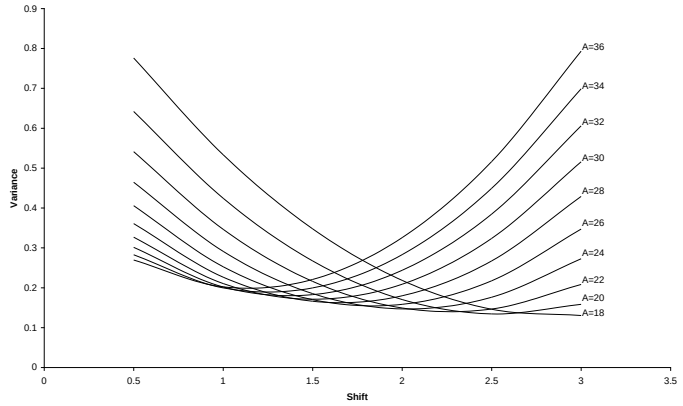

Figure 2.7 Graph of variance χ for $\hbar\omega = 14$, and $\alpha = 0.0500$ as a function of shift Δ in the diagonal two-body matrix elements

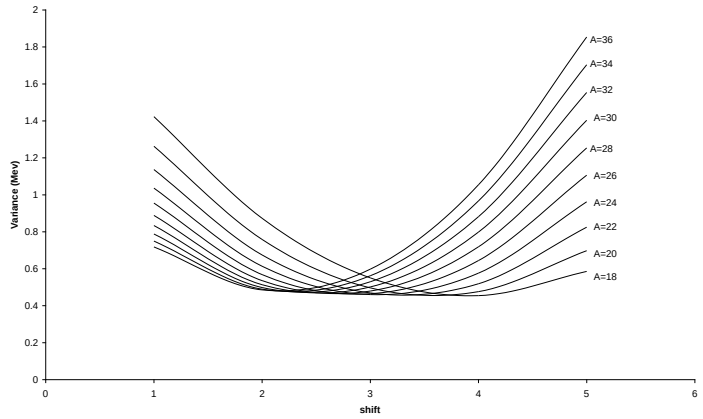

Figure 2.8 Graph of variance χ for $\hbar\omega = 14$, and $\alpha = 0.0000$ as a function of shift Δ in the diagonal two-body matrix elements

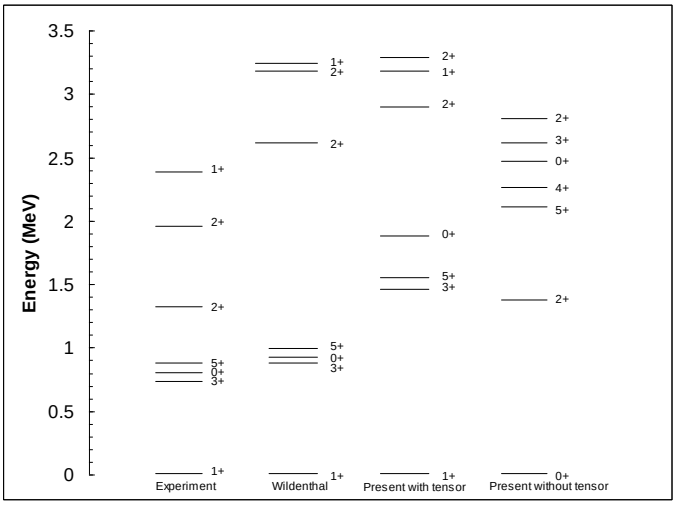

Figure 3.1 ^{18}F Energy Spectrum. $\hbar\omega = 13$, $\alpha = 0.0650$ (with tensor), $\alpha = 0.0000$ (without tensor)

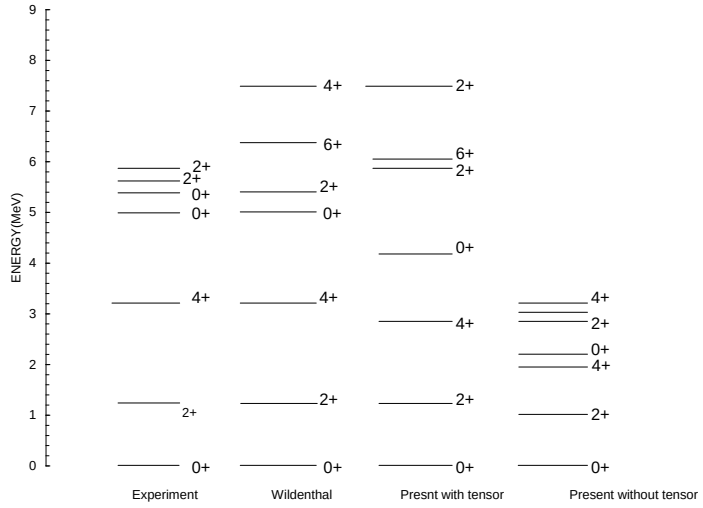

Figure 3.2 ^{20}Ne Energy Spectrum. $\hbar\omega = 13, \alpha = 0.0550$ (with tensor), $\alpha = 0.0000$ (without tensor)

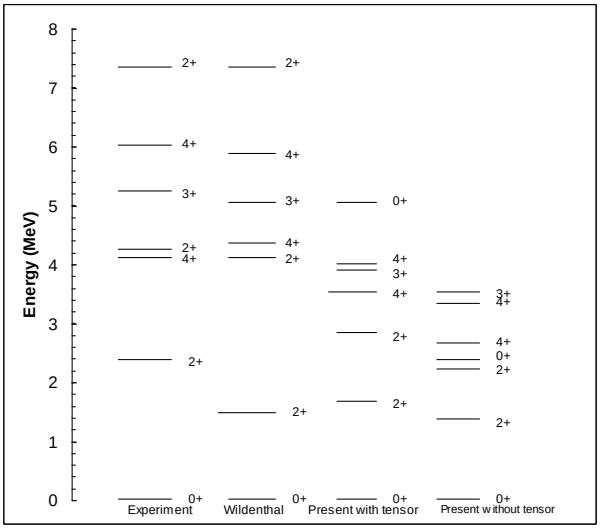

Figure 3.3 ^{24}Mg Energy Spectrum. $\hbar\omega = 13, \alpha = 0.0550$ (with tensor), $\alpha = 0.0000$ (without tensor)

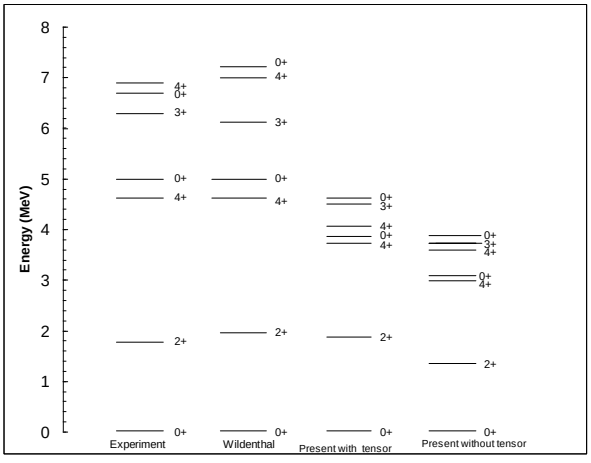

Figure 3.4 ^{28}Si Energy Spectrum. $\hbar\omega = 11, \alpha = 0.0550$ (with tensor), $\alpha = 0.0000$ (without tensor)

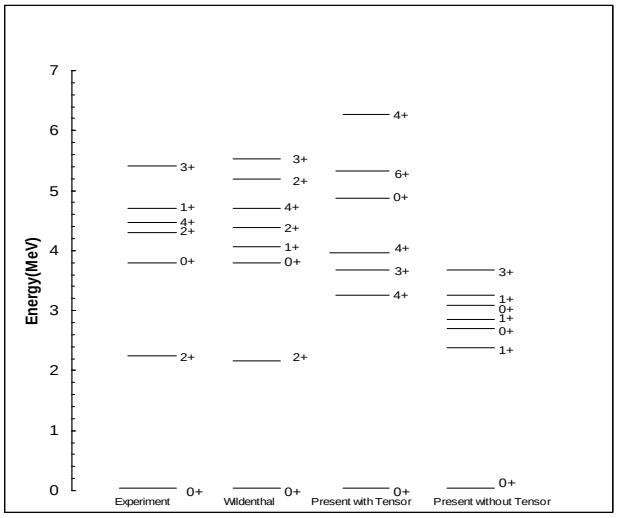

Figure 3.5 ^{32}S Energy Spectrum. $\hbar\omega = 11, \alpha = 0.0500$ (with tensor), $\alpha = 0.0000$ (without tensor)

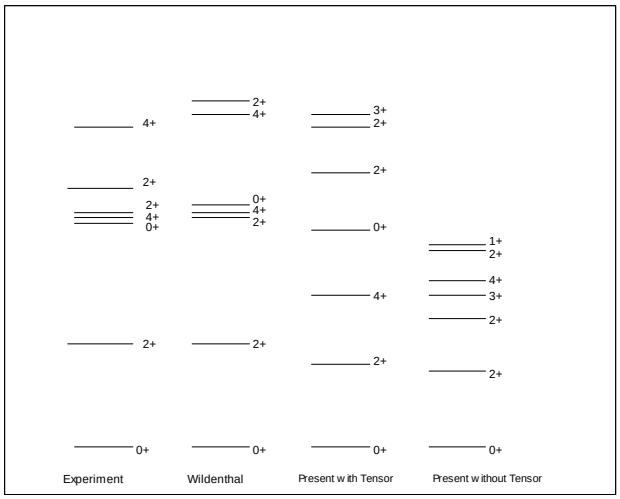

Figure 3.6 ^{36}Ar Energy Spectrum. $\hbar\omega = 11, \alpha = 0.0550$ (with tensor), $\alpha = 0.0000$ (without tensor)

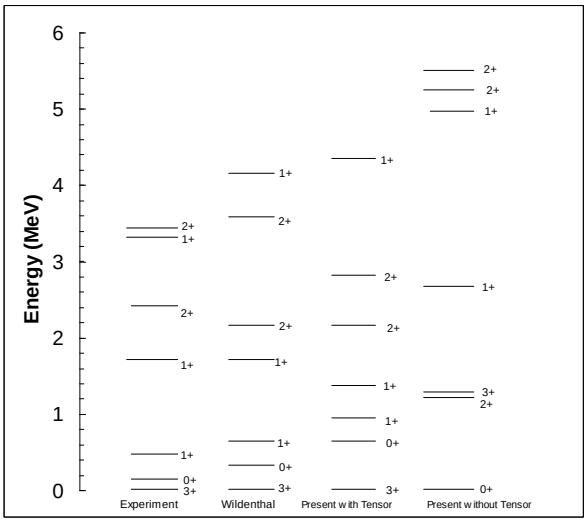

Figure 3.7 ^{38}K Energy Spectrum. $\hbar\omega = 11, \alpha = 0.0500$ (with tensor), $\alpha = 0.0000$ (without tensor)

References

[1] J.M. Irvine, G.S. Mani, V.F.E. Pucknell, M. Vallieres, and F. Yazici, (1976). Nuclear Shell-Model Calculations and strong two-body correlations. Ann. Phys. (N.Y.) **50**, 411.

[2] V.G.J. Stoks, R.A.M. Klamp, C.P.F. Terheggen, J.J. De Swart. (1994). Construction of high quality Nucleon-Nucleon Potential Models. Phys. Rev. **C49**, 2950

[3] J. M. Irvine,(1987). The Nuclear Matter Saturation Problem, Annales UMCS (Lublin, Poland) Section AAA XLII .

[4] J.O. Fiase, K.R.S. Devan, A. Hosaka. (2004).Binding energy and single particle energies in ^{16}O region. Phys. Rev **C66**, 014004

[5] J.M. Irvine, (1980). Constrained variational calcualtions for nuclear matter: N(1234) and the three-body calculations. Prog. Part. Nucl. Phys. **5**, 1

[6] J. Fiase, (2001). Mass dependence of single-particle energies for shell-model calculations. Phys. Rev. C **63**, 037303

[7] J. Fiase, A. Hamoudi, J.M. Irvin, F. Yazici: J. (1988). Effective interaction for sd-shell model calculaations. Phys. G. Nucl. Phys. **14**, 27

[8] M. Saha Sarkar, Abhijit Bisoi, Sudatta Ray, Ritesh Kshetri and S. Sarkar (2013). Understading nuclei in the upper sd-shell. Proc. DAE-BRN Symp. Nucl. Phys. (India).

[9] M. Saha Sarka, (2010). Evolution of sd-fp shell gap for upper sd shell nuclei. Proc. Of the DAE symp. On Nucl. Phys. Volume 55, pp119

[10] W. A. Ritcher and B. A. Brown. (2012). Review of nuclear structure calculations in the sd-shell for the rp process. Phys. Rev.C**85**045806

[11] http://www.nndc.bnl.gov. (2012).

[12] M. Bouhelal, F. Haa, E. Courier, F. Nowacki and A.Bouldjedri (2009). Negataive parity intruder states in sd-shell nuclei: A complete $1\hbar\omega$ shell model description. ACTA PHYSICAL POLONICA B Vol.40, No. 3, pp 639

[13] Wildenthal H.(1984) Emprircal strengths of spin operators in nuclei. Prog. Part. Nucl. Phys. **11** 5

[14] Ali K. Hassan and Fatema H. Obeed. (2013). Nuclear shell model application to calculate energy levels for nucleus $^{18}_{9}F_{9}$ by using Wildenthal interaction. *International Journal of Science and Research. Pp 2242* www.ijsr.net

[15] Saeed Mohammadi and Fatema Salimi (2015). Energy levels calculations of ^{30}Si ^{31}Si and Isotopes using OXBASH Code. American Journal of Modern Physics. Vol. 4, No. 3-1, pp40-43

[16] S. Mahammadi, A. Heydarzade and V. Ragheb. (2015). Energy levels calculation of $^{28,30}Si$ and $^{26,28}Al$ Isotopes using shell model code OXBASH. American Journal of Modern Physics. Vol. 4, No. 3-1, pp 32-35

[17] Saeed Mahammadi, Emad Zare Morzi and Nafiseh Shayan Shakib. (2016). Energy leveld calculations of potassium isotopes using OXBASH code. International Journa of Scientific Engineering and Applied Sciences (IJSEAS) Vol. 2 issue -11, pp72 – 75.